RESEARCH REPORTS
Biological

S.-K. Wang[1], Y. Hu[1], J.P. Simmer[1]*, F. Seymen[2], N.M.R.P. Estrella[3], S. Pal[1], B.M. Reid[1], M. Yildirim[2], M. Bayram[2], J.D. Bartlett[4], and J.C.-C. Hu[1]

[1]Department of Biologic and Materials Sciences, University of Michigan School of Dentistry, 1210 Eisenhower Place, Ann Arbor, MI 48108, USA; [2]Department of Pedodontics, University of Istanbul, Faculty of Dentistry, Istanbul, Turkey; [3]Department of Orthodontics and Pediatric Dentistry, University of Michigan School of Dentistry, Ann Arbor, MI, USA; and [4]Department of Cytokine Biology, The Forsyth Institute, Cambridge, MA, USA; *corresponding author, jsimmer@umich.edu

J Dent Res 92(3):266-271, 2013

Novel *KLK4* and *MMP20* Mutations Discovered by Whole-exome Sequencing

ABSTRACT

Non-syndromic amelogenesis imperfecta (AI) is a collection of isolated inherited enamel malformations that follow X-linked, autosomal-dominant, or autosomal-recessive patterns of inheritance. The AI phenotype is also found in syndromes. We hypothesized that whole-exome sequencing of AI probands showing simplex or recessive patterns of inheritance would identify causative mutations among the known candidate genes for AI. DNA samples obtained from 12 unrelated probands with AI were analyzed. Disease-causing mutations were identified in three of the probands: a novel single-nucleotide deletion in both *KLK4* alleles (g.6930delG; c.245delG; p.Gly82Alafs*87) that shifted the reading frame, a novel missense transition mutation in both *MMP20* alleles (g.15390A>G; c.611A>G; p.His204Arg) that substituted arginine for an invariant histidine known to coordinate a structural zinc ion, and a previously described nonsense transition mutation in a single allele of *FAM83H* (c.1379G>A; g.5663G>A; p.W460*). Erupted molars and cross-sections from unerupted parts of the mandibular incisors of *Mmp20* null mice were characterized by scanning electron microscopy. Their enamel malformations closely correlated with the enamel defects displayed by the proband with the *MMP20* mutation. We conclude that whole-exome sequencing is an effective means of identifying disease-causing mutations in kindreds with AI, and this technique should prove clinically useful for this purpose.

KEY WORDS: dental enamel, amelogenesis imperfecta, tooth, metalloproteases, serine proteases, human FAM83H protein.

DOI: 10.1177/0022034513475626

Received November 8, 2012; Last revision December 21, 2012; Accepted January 1, 2013

A supplemental appendix to this article is published electronically only at http://jdr.sagepub.com/supplemental.

INTRODUCTION

Non-syndromic amelogenesis imperfecta (AI) is a collection of inherited dental enamel malformations that can be caused by defects in many genes and can be manifested by diverse enamel phenotypes. X-linked AI is caused by defects in *AMELX*. Autosomal-dominant forms of AI can be caused by *ENAM* (Rajpar *et al*., 2001) and *FAM83H* (Kim *et al*., 2008) mutations, while autosomal-recessive AI can be caused by defects in *MMP20* (Kim *et al*., 2005), *KLK4* (Hart *et al.*, 2004), *WDR72* (El-Sayed *et al.*, 2009), and *C4orf26* (Parry *et al.*, 2012). These genes account for about half of all non-syndromic AI cases (Chan *et al*., 2011). The other causative genes are currently unknown.

The term 'amelogenesis imperfecta' is also used to describe the presence of an enamel phenotype in syndromes. Syndromic forms of AI and their associated causative genes include junctional epidermolysis bullosa (*LAMA3, LAMB3, LAMC2, COL17A1*) (Buchroithner *et al*., 2004; Almaani *et al*., 2009), cone-rod dystrophy and AI (*CNNM4*) (Parry *et al.*, 2009), AI with gingival fibromatosis syndrome (*FAM20A*) (O'Sullivan *et al.*, 2011), enamel-renal syndrome (*FAM20A*) (Wang *et al.*, in press), tricho-dento-osseous syndrome (*DLX3*) (Price *et al*., 1998), autoimmune polyendocrinopathy candidiasis ectodermal dystrophy (*AIRE*) (Pavlic and Waltimo-Sirén, 2009), oculodentodigital dysplasia (*GJA1*) (van Es *et al.*, 2007), and Kohlschütter-Tönz syndrome (*ROGDI*) (Schossig *et al.*, 2012), among others. Many of these conditions can be confused with non-syndromic forms of AI, since the enamel malformations may be the only apparent, or earliest-onset, phenotype in some cases.

As the number of candidate genes proven to cause inherited enamel defects has risen, genotype-phenotype correlations have been used to prioritize candidate genes for mutational analyses to identify the genetic defect. However, enamel phenotypes associated with many AI candidate genes are not distinctive, limiting the usefulness of genotype-phenotype correlations in predicting the causative gene, especially in recessive cases. Whole-exome sequencing identifies sequence variations in coding regions and intron junctions throughout the genome. Variations within candidate genes can then be analyzed to determine if they are disease-causing, and the results should prove useful in the diagnosis by dentists of patients with inherited disorders. In this study, we used whole-exome sequencing to identify disease-causing mutations in *KLK4, MMP20*, and *FAM83H* in our patients with amelogenesis imperfecta.

MATERIALS & METHODS

The human study protocol and participant consents were reviewed and approved by the Institutional Review Board at the University of Michigan. Study participants signed appropriate written consents after an explanation of their contents and after their questions about the study were answered. All animal procedures were approved by the University of Michigan Committee of Use and Care of Animals.

DNA Isolation and Characterization

Peripheral whole blood (5 cc) was obtained from recruited members of each family. Genomic DNA was isolated with the QIAamp DNA Blood Maxi Kit and protocol (Qiagen Inc., Valencia, CA, USA), and its quality and quantity were determined by spectrophotometry at OD_{260} and OD_{280}. DNA samples, one from each proband of the 12 AI kindreds showing a simplex or autosomal-recessive pattern of inheritance, were submitted for whole-exome sequencing (Edge BioSystems, Gaithersburg, MD, USA). Genomic DNA (3 μg) from each proband was nebulized into ~300-bp fragments, which were tailed and ligated to adapters, amplified, enriched, and analyzed by means of an Agilent 2100 Bioanalyzer prior to being sequenced in paired-end reads, 75 to 100 bases *per* read (Life Technologies SOLiD™ System, Carlsbad, CA, USA). For the 12 samples analyzed, the average depth of coverage of the targeted exome was 73x. The percentage of target bases not covered was 6.2%.

The annotated results were inspected to search for potential disease-causing sequence variations in the following candidate genes: *AMELX, ENAM, FAM83H, KLK4, MMP20, WDR72, FAM20A, C4orf26, CNNM4, AMBN, AMTN, ODAM, SP6, COL17A1, ROGDI, LAMA3, LAMB3, LAMC2, DLX3, GJA1, AIRE*, and *ABCC6*. In the three families with identified mutations, the exon carrying the suspected defect (*KLK4* coding exon 3, *MMP20* exon 4, and *FAM83H* exon 5) inclusive of adjoining intron sequences was amplified from all recruited family members and characterized by Sanger DNA sequencing.

Scanning Electron Microscopy (SEM)

Mandibular molars and incisors (sectioned at level 8 in the maturation stage and polished) from 9-week-old wild-type and *Mmp20* null mice were imaged with a Field Emission Gun Scanning Electron Microscope (FEG-SEM; Amray 1910 Field Emission Scanning Electron Microscope) at the Microscopy and Image Analysis Laboratory at the University of Michigan as described previously (Hu *et al*., 2011). Mandibular incisors (sectioned at level 3 at the end of the secretory stage) were examined by means of a Hitachi S-3000N variable pressure scanning electron microscope in backscatter mode as described previously (Smith *et al.*, 2011).

RESULTS

Family 1: *KLK4*

The proband (IV:1) of family 1 was a 9-year-old girl from Turkey with a hypomaturation form of amelogenesis imperfecta (Fig. 1) and no history of systemic disturbances. Her father (III:5) and mother (III:6) were first cousins (Fig. 1A), and their enamel appeared to be normal (Appendix Fig. 1). The enamel covering the proband's teeth appeared normal in size and shape, but was discolored brown, chipped on multiple teeth, and secondarily affected with dental caries (Fig. 1B). The proband had a class III molar relationship and may have lost vertical dimension. Although eruption of the maxillary incisors was delayed, there was no anterior open bite. Radiographically, the enamel was of normal thickness, but only slightly more radio-opaque than dentin (Fig. 1C). Whole-exome sequencing of the proband's genome identified a single-nucleotide deletion (g.6930delG; c.245delG; p.Gly82Alafs*87) in both *KLK4* alleles that shifted the reading frame at codon 82 of 255. The frameshift is in the third of 5 coding exons (Appendix Fig. 2), so the mutant *KLK4* mRNA transcripts might have been degraded by nonsense-mediated decay. If translated, the mutant protein would not be catalytically active, although it could potentially cause secondary pathology through dominant-negative or gain-of-function effects. The homozygous mutation was confirmed by Sanger sequencing of PCR amplification products. Both parents were heterozygous for the deletion (Fig. 1D). The simplex pattern of inheritance of the pedigree was thus shown to be autosomal-recessive.

Family 2: *MMP20*

The proband (III:2) of family 2 was a 14-year-old boy who was the only family member with a dental phenotype (Fig. 2A). His chief complaint concerned his dentition, which exhibited generalized hypoplastic (thin) enamel that abraded easily and was sensitive to thermal changes, particularly cold (Fig. 2B). Bitewing radiographs showed a thin enamel layer only slightly more radio-opaque than the underlying dentin. Whole-exome sequencing identified an apparent disease-causing mutation (g.15390A>G; c.611A>G; p.His204Arg) in both alleles of *MMP20* that was confirmed by Sanger sequencing. This sequence variation is absent from the dbSNP and 1000 Genomes Project Pilot Data databases. His^{204} coordinates a structural zinc ion (Maskos, 2005) and is conserved in all known *MMP20* sequences. The distribution of this sequence variation among the five members of the nuclear family was determined (Fig. 2C). The parents and the proband's younger brother (III:3) were heterozygous for the c.611A>G transition mutation, while the older brother had the wild-type sequence in both alleles. These analyses strongly support the conclusion that the homozygous *MMP20* p.His204Arg missense mutation caused the recessive enamel malformations in the proband.

Scanning electron microscopy of erupted first mandibular molars from 9-week-old *Mmp20* null mice showed severe abrasion of the occlusal surfaces (Fig. 3A). A polished, late-maturation-stage cross-section of an *Mmp20* null mouse mandibular incisor, where the enamel had reached full thickness but had not yet erupted and suffered abrasion, showed enamel thinner than that in the wild-type mouse (27 μm *vs*. 114 μm at the height of curvature) (Fig. 3B), and a smaller cross-sectional area (26,577 μm^2 *vs*. 70,389 μm^2). Backscatter SEMs of a polished cross-section

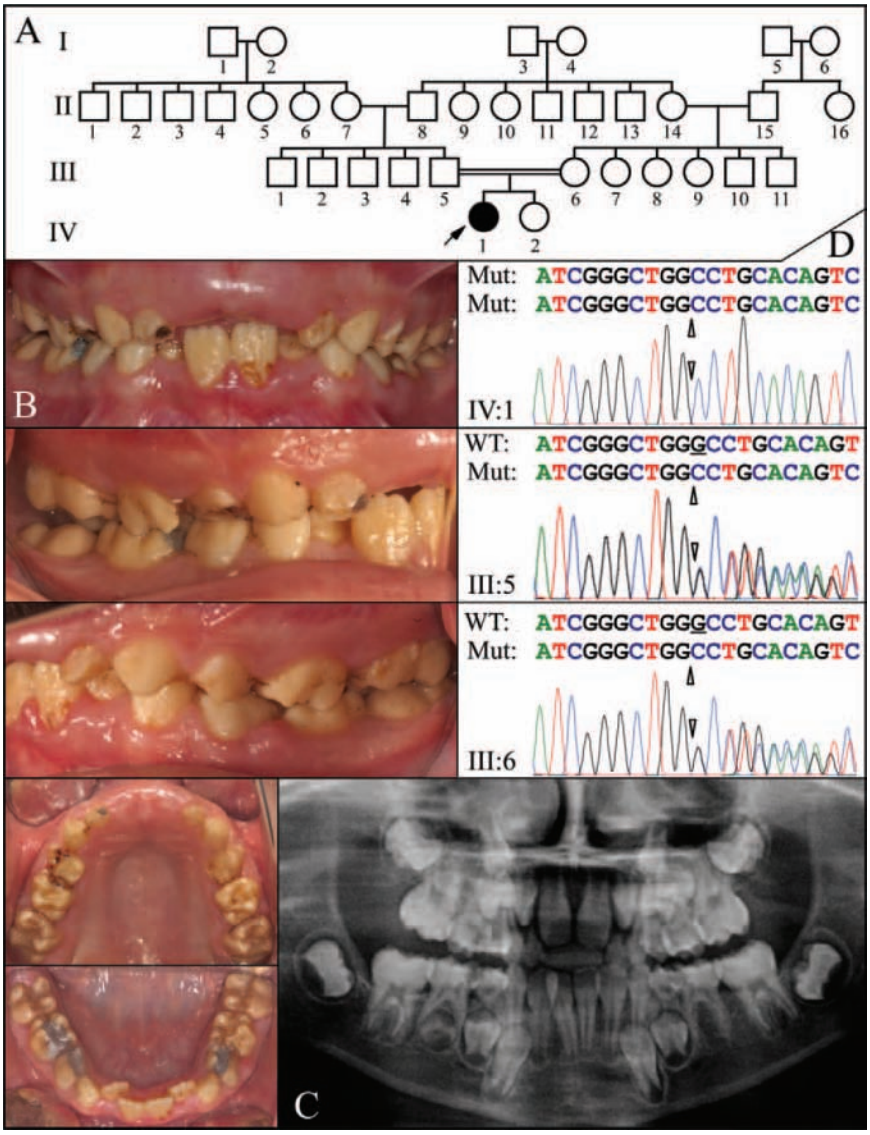

Figure 1. Family 1. (**A**) Pedigree of consanguineous family from Turkey with enamel malformations in the proband. (**B**) Frontal, lateral, and occlusal photos of the proband at age 9 yrs. The enamel is chipped and shaded brown. (**C**) Panorex radiograph of the mixed dentition showing enamel of normal thickness that contrasts only slightly with dentin. (**D**) DNA sequencing chromatograms showing that the single-nucleotide deletion (c.245delG; position marked by arrowhead) is homozygous in the proband and heterozygous in his parents.

of a mandibular incisor at the end of the secretory stage was already much thinner than that of the wild-type mouse and less mineralized in the deeper enamel near the dentin surface (Fig. 3C). The *Mmp20* null mouse enamel defects closely resemble those of the proband.

Family 3: *FAM83H*

The proband of family 3 was a 9-year-old Caucasian girl. The condition was reported to be inherited from the paternal side of her family. The proband's enamel was brown, soft with the consistency of hard cheese, did not contrast with dentin on radiographs, and abraded easily (Appendix Fig. 3). Oral hygiene was poor. Based upon her enamel phenotype, we screened *WDR72*, but no mutations were found. Whole-exome sequencing identified a heterozygous mutation in *FAM83H* (c.1379G>A; g.5663G>A; p.W460*) that was confirmed by Sanger sequencing. This mutation was previously shown to cause autosomal-dominant AI (Wright *et al.*, 2009), which is the reported pattern of inheritance in family 3, where a defect in a single *FAM83H* allele caused the enamel phenotype.

DISCUSSION

KLK4 is a serine proteinase that cleaves extracellular matrix proteins during the transition and maturation stages of amelogenesis (Lu *et al.*, 2008). *Klk4* null mice, with *lacZ* inserted in place of the *Klk4* coding region, have soft enamel that undergoes rapid attrition (Simmer *et al.*, 2009). No phenotype outside the dentition has been observed in these mice. Xgal staining of various tissues in the *lacZ* knock-in mice showed that *Klk4* is expressed at relatively high levels by maturation-stage ameloblasts and at trace levels in salivary glands and the prostate (Simmer *et al.*, 2011). Previously, a homozygous *KLK4* mutation introducing a premature stop codon was shown to cause hypomaturation AI in identical twins, with no signs or symptoms elsewhere in the body (Hart *et al.*, 2004). Disease-causing mutations in *KLK4* are extremely rare. This is only the second novel disease-causing *KLK4* mutation ever reported, although it has been a candidate gene for AI since it was originally cloned from developing teeth in the 1990s.

MMP20 is secreted by secretory- and early-maturation-stage ameloblasts (Hu *et al.*, 2002). The enzyme cleaves enamel extracellular matrix molecules, like amelogenin (Ryu *et al.*, 1999) and ameloblastin (Chun *et al.*, 2010). In the absence of MMP20, uncleaved enamel proteins accumulate in the secretory-stage enamel matrix (Yamakoshi *et al.*, 2011). Although a major function of MMP20 is to facilitate removal of enamel matrix proteins to enhance mineralization, the complex enamel phenotype that develops in its absence seems to involve the disruption of multiple processes.

Disease-causing mutations in *MMP20* are extremely rare. This is only the fifth novel disease-causing *MMP20* mutation reported to date (Appendix Fig. 4). In all cases, there was no evidence of systemic abnormalities. Although we observed

close similarity between the enamel malformations in our proband and those in *Mmp20* null mice, the enamel phenotypes observed in persons with different *MMP20* mutations vary (Appendix Fig. 4). Part of the variation in the enamel phenotypes may relate to the susceptibility of the malformed crowns to staining and abrasion following eruption. The enamel phenotype typically increases in severity with age, due to progressive deterioration.

FAM83H first came to the attention of scientists with the discovery that mutations in *FAM83H* cause autosomal-dominant hypocalcified amelogenesis imperfecta (ADHCAI) (Kim *et al*., 2008). *FAM83H* encodes an intracellular protein of unknown function that is associated with the Golgi apparatus or trans-Golgi network (Ding *et al*., 2009). To date, 20 novel *FAM83H* disease-causing mutations have been reported, and *all* are nonsense or frameshift mutations in the last coding exon that truncate the protein between Ser^{287} and Glu^{694} (Appendix Fig. 5). The N-terminal region of the mutant protein is all that is translated, sometimes along with a large frame-shifted segment. The N-terminal domain shares homology with the phospholipase D superfamily and is assumed to form dimers and to interact with other protein(s). Quaternary structures containing the truncated protein are thought to mediate dominant-negative effects in ameloblasts or their progenitors, and the resulting pathology causes enamel malformations.

Recently a single-nucleotide deletion in exon 5 of dog *Fam83h* showed no discernible phenotype in heterozygotes (Forman *et al.*, 2012). Even the homozygous mutants showed no obvious enamel abnormalities, but suffered from congenital keratoconjunctivitis sicca and ichthyosiform dermatosis (CKCSID), a disease not closely analogous to any human condition. The frameshift in dogs (c.977delC; p.Pro326Hisfs*258) is analogous to the types of mutations that cause ADHCAI in humans (Appendix Fig. 6). The dog results are mystifying. Perhaps the mutant FAM83H protein in dogs is degraded, or its mRNA transcript undergoes nonsense-mediated decay, so that the dominant-negative or gain-of-function effect is not observed.

MMP20 and KLK4 are the major extracellular proteases in developing enamel. When these enzymes were discovered, it was anticipated that defects in the genes encoding them might account for a high proportion of recessive AI cases, especially in families with hypomaturation AI, where the enamel shows normal thickness but is softer than normal and appears to contain residual enamel proteins. It now appears that defects in many genes cause autosomal-recessive AI. In this study, we were able to pinpoint the disease-causing mutation in three of 12 families by searching for mutations among a list of candidate genes. Since no probable disease-causing defects were observed among the many AI candidate genes in nine of the families, it is clear that more genes contribute to the etiology of autosomal-recessive AI than are currently recognized. This is consistent with recent studies reporting that mutational analyses of all the

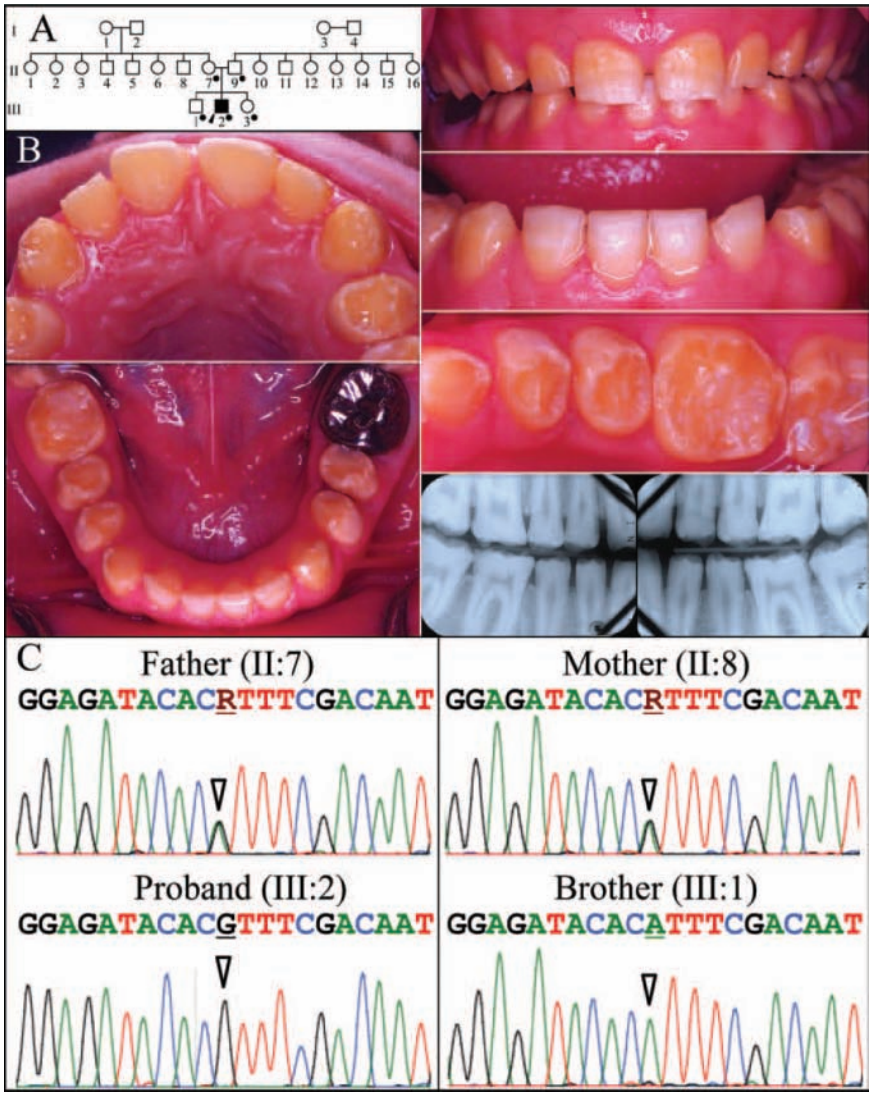

Figure 2. Family 2. (**A**) Pedigree of family with a simplex pattern of inheritance. DNA was obtained from the five persons in the nuclear family (black dots). (**B**) Oral photographs and bitewing radiographs of the proband at age 14 yrs. Most of the occlusal enamel had abraded from the mandibular first molars. The radiographs show a thin layer of enamel that is only slightly more radio-opaque than dentin. (**C**) DNA-sequencing chromatograms show that the parents were both heterozygous for the *MMP20* c.611A>G transition mutation, while the proband was homozygous for the mutation (p.His204Arg) and his older brother was homozygous-normal. The sequence analysis determined that the mutation was inherited in a recessive pattern.

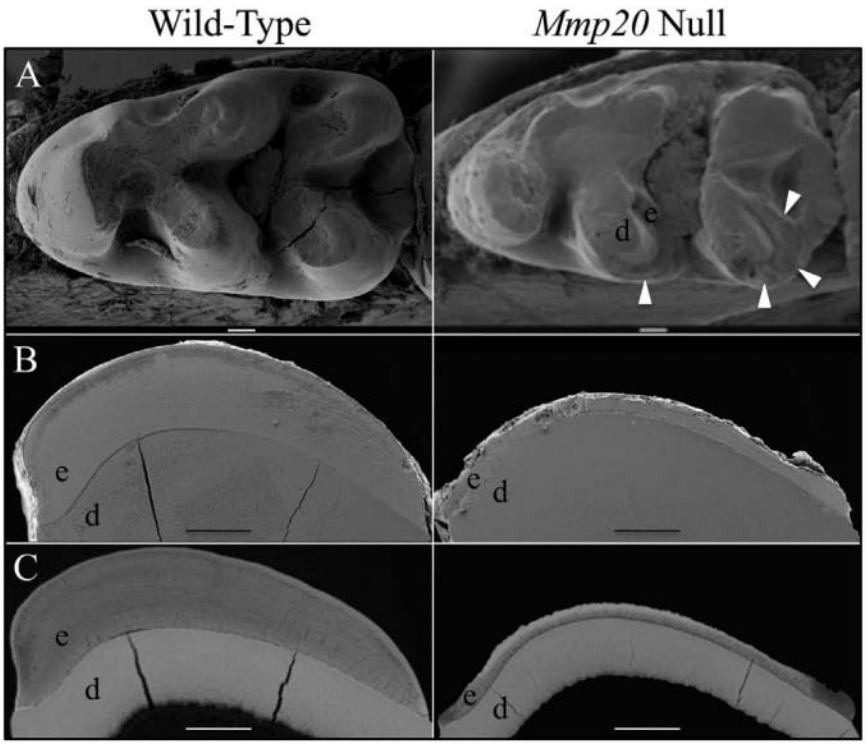

Figure 3. *Mmp20* null mouse enamel. **(A)** SEMs of occlusal surfaces of mouse first molars at 9 wks. The *Mmp20* null molar shows extensive abrasion, with enamel having chipped away from the biting surfaces (arrowheads). **(B)** SEM of mandibular incisors cross-sectioned at an unerupted location in the late-maturation stage. The *Mmp20* null enamel is only 1/3 as thick as that of the wild-type mouse. **(C)** SEM in backscatter mode of mandibular incisors cross-sectioned at a position near the transition from secretory to maturation stages. The *Mmp20* null enamel is thin, hypermineralized at the surface, but hypomineralized near the dentin. d, dentin; e, enamel. Bars = 100 μm.

known AI candidate genes cannot identify the disease-causing mutation in most recessive AI cases (Chan *et al*., 2011). Mutation analyses of known AI candidate genes identified the disease-causing mutation in only nine of 35 families with recessive AI (Wright *et al.*, 2011). Whole-exome sequencing is a rapidly evolving, high-throughput technology. It is possible that a disease-causing sequence variation was missed because of limitations of the sequencing platform and analysis pipeline; however, many common single-nucleotide polymorphisms (SNPs) were identified among the AI candidate genes in our study. Therefore, it is not because of the limitations of whole-exome sequencing that we identified the disease-causing mutation in only three of 12 probands, but because of our lack of knowledge of the full spectrum of genes that causes recessive forms of AI. Further analyses of the whole-exome sequences in these families may help us identify new AI candidate genes.

Recently, whole-exome sequencing added *FAM20A* (O'Sullivan *et al.*, 2011) and *C4orf26* (Parry *et al.*, 2012) to the list of candidate genes that causes syndromic and non-syndromic AI, respectively. Whole-exome sequencing is an efficient means of identifying the disease-causing mutation in kindreds with AI, as demonstrated in this report. Whole-exome sequencing makes it practical for dentists to consult clinical geneticists to order tests that can identify the disease-causing mutations in their patients with inherited enamel malformations to make a gene-based diagnosis of their type of AI and to determine whether or not systemic abnormalities should be anticipated.

ACKNOWLEDGMENTS

We thank the families in this study for their participation. This work was supported by the NIDCR/NIH (Grants DE019775, DE019622, and DE015846). The authors declare no potential conflicts of interest with respect to the authorship and/or publication of this article.

REFERENCES

Almaani N, Liu L, Dopping-Hepenstal PJ, Lovell PA, Lai-Cheong JE, Graham RM, *et al*. (2009). Autosomal dominant junctional epidermolysis bullosa. *Br J Dermatol* 160:1094-1097.

Buchroithner B, Klausegger A, Ebschner U, Anton-Lamprecht I, Pohla-Gubo G, Lanschuetzer CM, *et al*. (2004). Analysis of the LAMB3 gene in a junctional epidermolysis bullosa patient reveals exonic splicing and allele-specific nonsense-mediated mRNA decay. *Lab Invest* 84:1279-1288.

Chan HC, Estrella NM, Milkovich RN, Kim JW, Simmer JP, Hu JC (2011). Target gene analyses of 39 amelogenesis imperfecta kindreds. *Eur J Oral Sci* 119(Suppl 1):311-323.

Chun YH, Yamakoshi Y, Yamakoshi F, Fukae M, Hu JC, Bartlett JD, *et al*. (2010). Cleavage site specificity of MMP-20 for secretory-stage ameloblastin. *J Dent Res* 89:785-790.

Ding Y, Estrella MR, Hu YY, Chan HL, Zhang HD, Kim JW, *et al*. (2009). Fam83h is associated with intracellular vesicles and ADHCAI. *J Dent Res* 88:991-996.

El-Sayed W, Parry DA, Shore RC, Ahmed M, Jafri H, Rashid Y, *et al*. (2009). Mutations in the beta propeller WDR72 cause autosomal-recessive hypomaturation amelogenesis imperfecta. *Am J Hum Genet* 85:699-705.

Forman OP, Penderis J, Hartley C, Hayward LJ, Ricketts SL, Mellersh CS (2012). Parallel mapping and simultaneous sequencing reveals deletions in BCAN and FAM83H associated with discrete inherited disorders in a domestic dog breed. *PLoS Genet* 8:e1002462.

Hart PS, Hart TC, Michalec MD, Ryu OH, Simmons D, Hong S, *et al*. (2004). Mutation in kallikrein 4 causes autosomal recessive hypomaturation amelogenesis imperfecta. *J Med Genet* 41:545-549.

Hu JC, Sun X, Zhang C, Liu S, Bartlett JD, Simmer JP (2002). Enamelysin and kallikrein-4 mRNA expression in developing mouse molars. *Eur J Oral Sci* 110:307-315.

Hu Y, Hu JC, Smith CE, Bartlett JD, Simmer JP (2011). Kallikrein-related peptidase 4, matrix metalloproteinase 20, and the maturation of murine and porcine enamel. *Eur J Oral Sci* 119(Suppl 1):217-225.

Kim JW, Simmer JP, Hart TC, Hart PS, Ramaswami MD, Bartlett JD, *et al*. (2005). MMP-20 mutation in autosomal recessive pigmented hypomaturation amelogenesis imperfecta. *J Med Genet* 42:271-275.

Kim JW, Lee SK, Lee ZH, Park JC, Lee KE, Lee MH, *et al*. (2008). FAM83H mutations in families with autosomal-dominant hypocalcified amelogenesis imperfecta. *Am J Hum Genet* 82:489-494.

Lu Y, Papagerakis P, Yamakoshi Y, Hu JC, Bartlett JD, Simmer JP (2008). Functions of KLK4 and MMP-20 in dental enamel formation. *Biol Chem* 389:695-700.

Maskos K (2005). Crystal structures of MMPs in complex with physiological and pharmacological inhibitors. *Biochimie* 87:249-263.

O'Sullivan J, Bitu CC, Daly SB, Urquhart JE, Barron MJ, Bhaskar SS, *et al*. (2011). Whole-exome sequencing identifies FAM20A mutations as a cause of amelogenesis imperfecta and gingival hyperplasia syndrome. *Am J Hum Genet* 88:616-620.

Parry DA, Mighell AJ, El-Sayed W, Shore RC, Jalili IK, Dollfus H, *et al*. (2009). Mutations in CNNM4 cause Jalili syndrome, consisting of autosomal-recessive cone-rod dystrophy and amelogenesis imperfecta. *Am J Hum Genet* 84:266-273.

Parry DA, Brookes SJ, Logan CV, Poulter JA, El-Sayed W, Al-Bahlani S, *et al*. (2012). Mutations in C4orf26, encoding a peptide with in vitro hydroxyapatite crystal nucleation and growth activity, cause amelogenesis imperfecta. *Am J Hum Genet* 91:565-571.

Pavlic A, Waltimo-Sirén J (2009). Clinical and microstructural aberrations of enamel of deciduous and permanent teeth in patients with autoimmune polyendocrinopathy-candidiasis-ectodermal dystrophy. *Arch Oral Biol* 54:658-665.

Price JA, Bowden DW, Wright JT, Pettenati MJ, Hart TC (1998). Identification of a mutation in DLX3 associated with tricho-dento-osseous (TDO) syndrome. *Hum Mol Genet* 7:563-569.

Rajpar MH, Harley K, Laing C, Davies RM, Dixon MJ (2001). Mutation of the gene encoding the enamel-specific protein, enamelin, causes autosomal-dominant amelogenesis imperfecta. *Hum Mol Genet* 10:1673-1677.

Ryu OH, Fincham AG, Hu CC, Zhang C, Qian Q, Bartlett JD, *et al*. (1999). Characterization of recombinant pig enamelysin activity and cleavage of recombinant pig and mouse amelogenins. *J Dent Res* 78:743-750.

Schossig A, Wolf NI, Fischer C, Fischer M, Stocker G, Pabinger S, *et al*. (2012). Mutations in ROGDI cause Kohlschütter-Tönz Syndrome. *Am J Hum Genet* 90:701-707.

Simmer JP, Hu Y, Lertlam R, Yamakoshi Y, Hu JC (2009). Hypomaturation enamel defects in Klk4 knockout/LacZ knockin mice. *J Biol Chem* 284:19110-19121.

Simmer JP, Richardson AS, Smith CE, Hu Y, Hu JC (2011). Expression of kallikrein-related peptidase 4 in dental and non-dental tissues. *Eur J Oral Sci* 119(Suppl 1):226-233.

Smith CE, Richardson AS, Hu Y, Bartlett JD, Hu JC, Simmer JP (2011). Effect of kallikrein 4 loss on enamel mineralization: comparison with mice lacking matrix metalloproteinase 20. *J Biol Chem* 286:18149-18160.

van Es RJ, Wittebol-Post D, Beemer FA (2007). Oculodentodigital dysplasia with mandibular retrognathism and absence of syndactyly: a case report with a novel mutation in the connexin 43 gene. *Int J Oral Maxillofac Surg* 36:858-860.

Wang SK, Aref P, Hu Y, Milkovich RN, Simmer JP, El-Khateeb M, *et al*. (2013). FAM20A mutations can cause Enamel-Renal Syndrome (ERS). *PLoS Genet* (in press).

Wright JT, Frazier-Bowers S, Simmons D, Alexander K, Crawford P, Han ST, *et al*. (2009). Phenotypic variation in FAM83H-associated amelogenesis imperfecta. *J Dent Res* 88:356-360.

Wright JT, Torain M, Long K, Seow K, Crawford P, Aldred MJ, *et al*. (2011). Amelogenesis imperfecta: genotype-phenotype studies in 71 families. *Cells Tissues Organs* 194:279-283.

Yamakoshi Y, Richardson AS, Nunez SM, Yamakoshi F, Milkovich RN, Hu JC, *et al*. (2011). Enamel proteins and proteases in Mmp20 and Klk4 null and double-null mice. *Eur J Oral Sci* 119(Suppl 1):206-216.